Available online at www.sciencedirect.com

ScienceDirect

www.elsevier.com/locate/jes

JES JOURNAL OF ENVIRONMENTAL SCIENCES

www.jesc.ac.cn

# A mechanistic study of ciprofloxacin adsorption by goethite in the presence of silver and titanium dioxide nanoparticles

*Jie Tang*[1,2], *Yun Wang*[1,2], *Qiang Xue*[1,2,*], *Fei Liu*[1,2], *Kenneth C. Carroll*[3,4], *Xiaohua Lu*[5], *Taogeng Zhou*[6], *Dengjun Wang*[7]

[1] *MOE Key Laboratory of Groundwater Circulation and Environmental Evolution, China University of Geosciences (Beijing), Beijing 100083, China*
[2] *Beijing Key Laboratory of Water Resources and Environmental Engineering, School of Water Resources and Environment, China University of Geosciences (Beijing), Beijing 100083, China*
[3] *Water Science and Management Program, New Mexico State University, MSC 3Q, USA*
[4] *Plant & Environmental Science, New Mexico State University, Las Cruces, NM 88003, USA*
[5] *National Institute of Metrology, Beijing 100022, China*
[6] *Beijing Institute of Technology, Beijing 100081, China*
[7] *School of Fisheries, Aquaculture and Aquatic Sciences, Auburn University, Auburn, AL 36849, USA*

ARTICLE INFO

*Article history:*
Received 26 June 2021
Revised 28 August 2021
Accepted 29 August 2021
Available online 10 January 2022

*Keywords:*
Ciprofloxacin
Goethite
Silver nanoparticles
Titanium dioxide nanoparticles
Adsorption

ABSTRACT

The adsorption behaviors of ciprofloxacin (CIP), a fluoroquinolone antibiotic, onto goethite (Gt) in the presence of silver and titanium dioxide nanoparticles (AgNPs and $TiO_2$NPs) were investigated. Results showed that CIP adsorption kinetics in Gt with or without NPs both followed the pseudo-second-order kinetic model. The presence of AgNPs or $TiO_2$NPs inhibited the adsorption of CIP by Gt. The amount of inhibition of CIP sorption due to AgNPs was decreased with an increase of solution pH from 5.0 to 9.0. In contrast, in the presence of $TiO_2$NPs, CIP adsorption by Gt was almost unchanged at pHs of 5.0~6.5 but was decreased with an increase of pH from 6.5 to 9.0. The mechanisms of AgNPs and $TiO_2$NPs in inhibiting CIP adsorption by Gt were different, which was attributed to citrate coating of AgNPs resulting in competition with CIP for adsorption sites on Gt, while $TiO_2$NPs could compete with Gt for CIP adsorption. Additionally, CIP was adsorbed by Gt or $TiO_2$NPs through a tridentate complex involving the bidentate inner-sphere coordination of the deprotonated carboxylic group and hydrogen bonding through the adjacent carbonyl group on the quinoline ring. These findings advance our understanding of the environmental behavior and fate of fluoroquinolone antibiotics in the presence of NPs.



## Introduction

Fluoroquinolones (FQs), a class of antibiotics commonly used in humans and animals, has been frequently detected in

* Corresponding author.
*E-mail:* xueqiang@cugb.edu.cn (Q. Xue).

https://doi.org/10.1016/j.jes.2021.08.052
1001-0742/

water and soil environment, because more than 75% of the dosage of antibiotics used can be discharged through feces and urine (Golet et al., 2001; Valdes et al., 2021). The FQs remaining in the environment can cause development of bacterial antibiotic resistance, which would affect the treatment of disease and increase health risks. To decrease the potential risks, FQs compounds have been listed as priority control substances (Pico and Andreu, 2007; Gonzalez-Pleiter et al., 2013; Coulibaly et al., 2020). Currently, ciprofloxacin (CIP) is one of the most widely used FQs globally (Pico and Andreu, 2007), and it has a strong antibacterial activity on both Gram-positive and Gram-negative bacteria (Davis et al., 1996). It has been reported that the concentrations of CIP detected in wastewater treatment plants (WWTPs) effluent, surface water, groundwater and sediment have reached 31 mg/L, 6.5 mg/L, 0.014 mg/L, and 20 mg/kg, respectively (Larsson et al., 2007; Van Doorslaer et al., 2014; Kovalakova et al., 2020).

Adsorption plays an important role in controlling the environmental fate of FQs. Over the past decade, a number of studies on the adsorption of CIP by various minerals and soils, including hematite (Martin et al., 2015; Zhou et al., 2019), goethite (Gt) (Gu et al., 2015; Tan et al., 2014), montmorillonite (Wang et al., 2010; Wu et al., 2019), sludge (Li and Zhang, 2010; Zhang et al., 2019a) and sediment (Mutavdzic Pavlovic et al., 2017; Huang et al., 2020), have been investigated. Among these, Gt is one of the most common and stable iron hydroxides in nature, which has been received widespread attention. Previous results suggested that CIP adsorption by Gt was highly dependent on pH, and higher adsorption was found with lower solution pH or higher ionic strength conditions (Gu et al., 2015). CIP and Gt can form bidentate chelates only involving both oxygens of the carboxylic group (Trivedi and Vasudevan, 2007), which was different from the complexation model of CIP adsorbed onto hydrous ferric oxides as proposed by Gu and Karthikeyan (Gu and Karthikeyan, 2005). Subsequently, there was also hydrogen bonding through the adjacent carbonyl group on the quinoline ring in the complexation between CIP and Gt (Gu et al., 2015). Additionally, divalent cations or fulvic acid introduced could obviously enhance the CIP adsorption by Gt, and the complexation of CIP on Gt in the presence of Cu(II) was observed to form a six-member ring between Cu and the oxygen of deprotonated carboxylic group and adjacent carbonyl group on the quinoline ring (Gu et al., 2015; Tan et al., 2014).

With the rapid development of nanotechnology, various nanoparticles (NPs) have been widely used in many fields, such as automobile, electronics, cosmetics and pharmaceuticals, which has resulted in their wide dissemination in surface water, WWTPs, and sewage sludge (Bundschuh et al., 2018; Zhang et al., 2019b; Nowack and Bucheli, 2007). The interaction between NPs and FQs has received widespread attention, especially for the most commonly used metal/metal oxide NPs in commercial products such as silver and titanium dioxide nanoparticles (AgNPs or $TiO_2$NPs) (Musee, 2017). For example, prior studies have found enoxacin replaced citrate molecule that prevented aggregation of AgNPs, increased their dispersion, and formed complex with AgNPs (Deng et al., 2016; Tyagi and Kumar, 2020). Furthermore, a recent study indicated that ofloxacin (OFL) could be adsorbed and degraded to de-methylated and de-carboxylated FQs by $TiO_2$NPs, especially at solution pH where OFL was zwitterionic (Van Wieren et al., 2012). However, adsorption of FQs on the $TiO_2$ surface is a prerequisite for degradation (Paul et al., 2010). Therefore, Paul et al (2012) proposed a surface complexation model, a tridentate mode of adsorption involving the bidentate innersphere coordination of the deprotonated carboxylic group and hydrogen bonding through the adjacent carbonyl group on the quinoline ring, to describe the adsorption behavior of OFL by $TiO_2$NPs.

**Table 1 – The physicochemical properties of Gt, AgNPs and $TiO_2$NPs.**

| Name | $pH_{PZC}$ | SSA ($m^2$/g) | Mean particle size (nm) |
|---|---|---|---|
| Gt | 9.4[a] | 93.45[a] | - |
| AgNPs | <2[b] | - | 20[c] |
| $TiO_2$NPs | 6.9[a] | 50~55 [c] | 21[c] |

a: Measured in this study; b: Literature reported data, the citrate-coated AgNPs were reported to be negatively charged at pHs range of 2~10 (El Badawy et al., 2011); c: Provided by the vendor.
$pH_{PZC}$: pH of point of zero charge; SSA: Specific surface area.

It is clear that NPs are also becoming co-located with CIP and other FQs (through wastewater treatment plant and other effluent discharges). The sorption processes of contaminant mixtures can become more uncertain and complex, and this can be the case for various mixtures of water contaminants such as NPs and antibiotics when they are co-located. Mixtures of contaminants also tend to have more uncertainty in multicomponent transport, reactivity, and biological toxicity. Thus, it is necessary to examine the mixture impacts on adsorption and transport of water contaminants including antibiotics and NPs. In this work, the adsorption behaviors of CIP onto a Gt surface in the presence of AgNPs and $TiO_2$NPs were carefully characterized by batch adsorption experiments and spectroscopic techniques. The main objectives are to illuminate the difference between the effects of AgNPs and $TiO_2$NPs on CIP adsorption by Gt and reveal its mechanism. These results advance our understanding of the environmental fate of CIP and other FQs in the presence of NPs.

## 1. Materials and methods

### 1.1. *Materials*

Gt was synthesized according to published methods (Hiemstra et al., 1989). AgNPs (Number XFJ6385-60-9 and Batch 100957) coated with citrate was supplied by XFNANO, China. $TiO_2$NPs (Type P25) was developed by Degussa Company, German. The point of zero charge (PZC) of Gt or $TiO_2$NPs were determined by microelectrophoresis (NanoSizer ZEN2600, Malvern, UK), and the specific surface area (SSA) of Gt was measured using the BET method (Micrometer, ASAP2460, USA). The physicochemical properties of Gt, AgNPs and $TiO_2$NPs are displayed in **Table 1**. CIP (purity > 98%) was purchased from Sigma-Aldrich, USA, and stored at -20°C prior to use. Unless otherwise noted, all chemicals used in this

study were of analytical grade or higher, and all solutions were prepared using ultrapure water (Millipore Corp, USA).

### 1.2. Batch experiments

To investigate and compare the effect of NPs on adsorption of CIP onto Gt, five sets of experiments were designed, including Gt-CIP (CIP adsorbed onto Gt), AgNPs-CIP (CIP adsorbed onto AgNPs), $TiO_2$NPs-CIP (CIP adsorbed onto $TiO_2$NPs), Gt-AgNPs-CIP (effect of AgNPs on adsorption of CIP onto Gt), and Gt-$TiO_2$NPs-CIP (effect of $TiO_2$NPs on adsorption of CIP onto Gt).

The effect of NPs concentration was evaluated using transient mixed reactor experiments, including 5 different reaction systems (Gt-CIP, $TiO_2$NPs-CIP and Gt-$TiO_2$NPs-CIP). The order of reagent addition to the 40 mL brown glass vials was as follows: Gt was weighted into vials, and then NP-aqueous suspension and CIP aqueous solution (pH = 6.5, 0.1 mol/L NaCl background electrolyte) were added in turn. The concentration of CIP and AgNPs were both 0.5 mg/L and 0.5 mg/L, and the concentration of $TiO_2$NPs were 0.5 mg/L, 5 mg/L, and 500 mg/L, respectively, and the suspension density of Gt was 1 g/L. The pH of CIP solution was adjusted using HCl and NaOH solutions (0.01, 0.05, and 0.1 mol/L). The reactor vials were shaken for 300 min on a rotator at a rate of 175 r/min at 25 °C in the dark. Subsequently, the samples were centrifuged at 3000 r/min for 5 min, and then the supernatants were centrifuged using a high-speed centrifuge at 12,000 r/min for 15 min. The supernatants from centrifugation were collected for analysis of the CIP concentration.

According to the results of NPs concentration, experiments for adsorption kinetics with or without NPs were conducted under the same experimental conditions as the NPs concentration experiment. The concentration of NPs were 0.5 mg/L AgNPs and 500 mg/L $TiO_2$NPs, respectively. In addition, subsamples were collected from the reactor vials after shaking for 5, 10, 20, 40, 60, 180, and 300 min.

Aqueous speciation of CIP and surface charge on the solid-phase are effected by the pH in solution. So, experiments that were focused on evaluating the effect of pH variability on CIP adsorbed were carried out similarly as detailed above, except that the series of experiment reaction solutions had pH values including 5.0, 6.0, 7.0, 8.0, or 9.0, respectively. The pH was adjusted by HCl and NaOH solution additions (0.01, 0.05 and 0.1 mol/L), and reaction time for these experiments was 300 min.

To further elucidate the mechanism of CIP adsorption by Gt in the presence of $TiO_2$NPs, the experiment of CIP initial concentration on CIP adsorbed onto Gt was conducted similarly as detailed above. The initial concentration of CIP aqueous solution (pH=6.5, 0.1 mol/L NaCl background electrolyte) were 0.4, 0.5, 0.6, 0.7, 0.8, 0.9 and 1 mg/L, respectively.

In this study, the above experiments were conducted in triplicate ($n = 3$) to ensure reliable results. Additionally, blank and control samples without CIP and control samples without Gt were also conducted.

### 1.3. Chemical analysis

The concentration of CIP in solution was measured using the high-performance liquid chromatography (HPLC) (LC-1220, Agilent, USA) with an Inertsil® SB-Aq column (4.6 mm × 150 mm, 5 μm particle size). The HPLC was equipped with variable wavelength detector, and detection wavelength was set to 278 nm (Pellegrino et al., 2008). The column temperature was maintained at 30 °C. 10 μL samples were injected through the autosampler, and the mobile phase flow rate was 1.0 mL/min with 25/75% (V/V) acetonitrile / potassium dihydrogen phosphate (25 mmol/L, pH = 2.5). The lower detection limit of the test was 53.8 $\mu$g/L. No CIP was detected in bank samples and the relative error of duplicates was controlled within 7%.

### 1.4. Data analysis

The amounts of CIP adsorbed were calculated by the following equation:

$$q_t = \frac{C_0 - C_t}{M} \cdot V \tag{1}$$

Where $q_t$ is the amount of CIP adsorbed onto solid-phase at time t, mg/g; $C_0$ and $C_t$ are CIP concentrations in aqueous-phase at initial time and time t, respectively, mg/L; M is the mass of solid-phase, g; and V is the volume of aqueous-phase, L.

To investigate the adsorption process, the pseudo-first-order kinetic model and the pseudo-second-order kinetic model were employed to simulate the experimental data (Oshannessy and Winzor, 1996; Simonin, 2016; Ho, 2006), which could be expressed as below:

Pseudo-first-order kinetic model:

$$q_t = q_e\left(1 - e^{-k_1 t}\right) \tag{2}$$

$$\ln(q_e - q_t) = \ln q_e - k_1 t \tag{3}$$

Pseudo-second-order kinetic model:

$$q_t = \frac{q_e^2 k_2 t}{1 + q_e k_2 t} \tag{4}$$

$$h = k_2 q_e^2 \tag{5}$$

Where $t$ is reaction time, min; $q_t$ and $q_e$ are the amount of CIP adsorbed onto solid-phase at time $t$ and equilibrium, mg/g; $k_1$ and $k_2$ is the adsorption rate constant, 1/min and mg/g/min, respectively; and $h$ is the initial adsorption rate constant, g/mg/min.

In order to ascertain the influencing level of AgNPs or $TiO_2$NPs on CIP adsorbed by Gt, Eq. (6) was used to calculate as below:

$$\eta = \frac{C_2 - C_1}{C_1} \times 100\% \tag{6}$$

Where $|\eta|$ is the influence level of AgNPs or $TiO_2$NPs on the adsorption of CIP onto Gt; $C_1$ is CIP concentration remaining in Gt-CIP, mg/L; and $C_2$ is CIP concentration remaining in Gt-AgNPs-CIP or Gt-$TiO_2$NPs-CIP, mg/L, respectively.

### 1.5. *Spectroscopic analysis*

Samples for Fourier-Transform Infrared (FTIR) spectrometer analysis were collected from the following experiments. Similar to previous studies (Gu et al., 2015), the solid/liquid ratio of Gt was increased from 1:1000 in batch experiments to 1:250, and CIP initial concentration was increased from 0.5 mg/L to 500 mg/L, and background electrolyte was still 0.1 mol/L NaCl. Samples were prepared at pH = 5, 7, and 9, respectively. Experiments included the CIP solution, Gt-CIP and $TiO_2$NPs-CIP binary systems, and Gt-$TiO_2$NPs-CIP ternary system. When reaction time reached 300 min, suspensions were separated with centrifugation, and the wet pastes were dried at 45 °C for 48 hr. Then the samples were mixed with KBr at a ratio of 1:10 prior to testing. IR spectrometer (Nicolet IS10, USA) was used to observe the infrared spectra of samples, operated in the wavenumber range of 400~4000 $cm^{-1}$ at 4 $cm^{-1}$ resolution.

Samples prepared for X-ray photoelectron spectroscopy (XPS) analysis were prepared from Gt-AgNPs-CIP ternary system, including 1 g/L Gt, 0.5 mg/L CIP, 0.1 mol/L NaCl, 0.5 mg/L or 20 mg/L AgNPs, and solution pH=6.5. The reaction time of Gt-0.5 mg/L AgNPs-CIP ternary system was 300 min, while Gt-20 mg/L AgNPs-CIP ternary system were 5 min, 10 min and 300 min, respectively. After reaction, suspensions were separated upon standing for 20 min, the wet pastes were freeze-dried at 48 hr, and then crushed to ensure homogeneity prior to testing. The XPS spectra of samples were obtained from a Thermo Scientific ESCALAB 250XI. Testing conditions and parameters were consistent with previous research (Hu et al., 2019). CasaXPS software was used to split peaks and also used for fitting to the data (Yang et al., 2019).

## 2. Results and discussion

### 2.1. *Adsorption kinetics*

The effect of NPs concentrations on CIP adsorbed onto Gt was conducted prior to studying adsorption kinetics, as shown in **Fig. 1**. It is observed that CIP is not adsorbed by 0.5 mg/L AgNPs, but the amount of CIP adsorbed onto Gt was reduced by 11.21%. Furthermore, CIP concentrations remaining in the $TiO_2$NPs-CIP binary system and Gt-$TiO_2$NPs-CIP ternary system were decreased with increasing the $TiO_2$NPs concentration. When the $TiO_2$NPs concentrations were 0.5 mg/L, 5 mg/L and 500 mg/L, the adsorption rate of CIP in Gt-$TiO_2$NPs-CIP was 1.03%, 10.73% and 35.33% more than in Gt-CIP, respectively. Therefore, 0.5 mg/L AgNPs and 500 mg/L $TiO_2$NPs was used for all of the follow-up experiment to better observe and quantify the difference while also exploring the mechanism of CIP adsorption by Gt in the presence of NPs.

The adsorption processes of CIP on three systems (Gt-CIP, Gt-AgNPs-CIP and Gt-$TiO_2$NPs-CIP) are shown in **Fig. 2a**. CIP was initially adsorbed quickly onto Gt and $TiO_2$NPs surfaces in the rest of systems, and then CIP transitioned more slowly as it reached equilibrium at 300 min, which was similar with phenomenon of fluoroquinolone antibacterial agents (FQs) adsorbed onto Gt (Zhang and Huang, 2007). The amounts of CIP adsorbed in Gt-CIP, Gt-AgNPs-CIP and Gt-$TiO_2$NPs-CIP reached

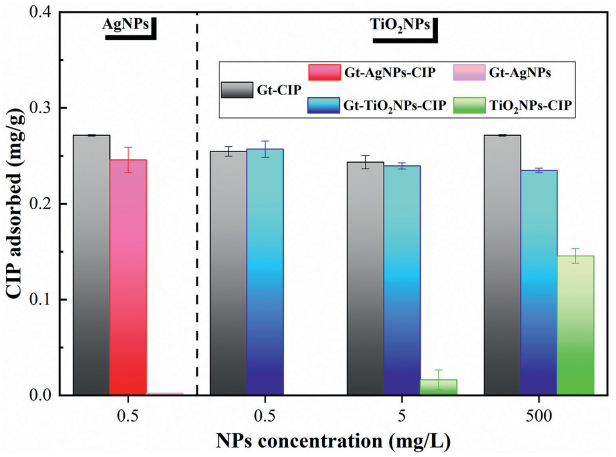


**Fig. 1 – Effect of NPs on CIP absorption. The concentrations of CIP is 0.5 mg/L, the background electrolyte is 0.1 mol/L NaCl, the suspension density of Gt is 1 g/L, and solution pH is 6.5. (Error bars represent standard deviation of $n = 3$ measurements).**

a constant level of 0.271 mg/g, 0.238 mg/g and 0.235 mg/g, respectively. Clearly, citrate coated AgNPs inhibited CIP adsorption by Gt. A previous study has shown that citrate can compete for adsorption sites of Gt and form inner/outer-sphere complex under the different pH conditions (Lindegren et al., 2009). Similarly, the amount of CIP adsorbed in Gt-$TiO_2$NPs-CIP was less than in Gt-CIP, which might be due to the competition adsorption of CIP by $TiO_2$NPs (**Fig. 1**). Overall, introducing AgNPs or $TiO_2$NPs in the study concentration inhibited CIP adsorption onto Gt.

As shown in **Fig. 2b**, the $\ln(q_e - q_t)$ and time did not produce a linear relationship, which indicated that the kinetic experimental data was not well fitted by the pseudo-first-order kinetic model. However, it was observed in **Fig. 2a** and **Table 2** that pseudo-second-order kinetic model could fit the CIP adsorption process well ($R^2 > 0.999$, $P(\text{prob}>F) < 10^{-9}$), and $q_e^{exp}$ was similar to $q_e^{cal}$ values that were estimated by the pseudo-second-order kinetic model. These results indicated that the CIP adsorption behavior was composed of multiple adsorption processes, but dominated by chemisorption (Ho, 2006). Moreover, the adsorption rate constants ($k_2$) for CIP adsorption in Gt-CIP, Gt-AgNPs-CIP and Gt-$TiO_2$NPs-CIP were 3.22 g/mg/min, 1.76 g/mg/min and 4.01 g/mg/min, respectively. It was observed that the magnitudes of $k_2$ in the different systems were in order of Gt-$TiO_2$NPs-CIP > Gt-CIP > Gt-AgNPs-CIP. Clearly from these results, NPs were observed to have a significant effect on $k$ in CIP adsorption by Gt. Thus, $TiO_2$NPs can compete with goethite to adsorb CIP in aqueous solutions. Also, citrate coated AgNPs competed with CIP for the adsorption sites of Gt, which we attribute to be the reason for the difference between them.

### 2.2. *Effect of solution pH*

The effects of solution pH variations on CIP adsorption under different conditions are shown in **Fig. 3a**. CIP concentration in the AgNPs-CIP binary system was essentially unchanged

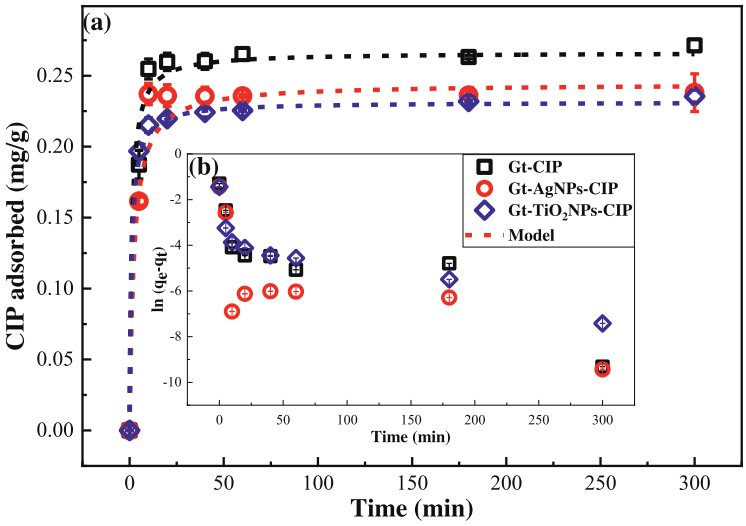


**Fig. 2 – (a) Effect of reaction time on CIP absorption under the different conditions and fitting curves of adsorption kinetic equation using pseudo-second-order kinetic model; (b) Fitting curves of adsorption kinetic equation using pseudo-one-order kinetic model. The concentrations of CIP, AgNPs and $TiO_2$NPs are 0.5 mg/L, 0.5 mg/L and 500 mg/L, respectively, the background electrolyte is 0.1 mol/L NaCl, the suspension density of Gt is 1 g/L, and solution pH is 6.5. (Measured data are symbols and simulation results presented as dotted lines, error bars represent standard deviation of $n = 3$ measurements).**

**Table 2 – Adsorption rate constants and equilibrium adsorption amounts of CIP associated with pseudo-second-order kinetic model.**

| Parameters Conditions | $q_e^{exp}$ (mg/g) | $q_e^{cal}$ (mg/g) | K (g/mg/min) | H (mg/g/min) | $R^2$ | P (prob>F) |
|---|---|---|---|---|---|---|
| Gt-CIP | 0.271 | 0.266 | 3.22 | 0.23 | 0.9996 | 1.1E-10 |
| Gt-AgNPs-CIP | 0.238 | 0.244 | 1.76 | 0.11 | 0.9992 | 9.2E-10 |
| Gt- $TiO_2$NPs-CIP | 0.235 | 0.231 | 4.01 | 0.21 | 0.9999 | 1.3E-13 |

$q_e^{exp}$ and $q_e^{cal}$ are the equilibrium adsorption amount of experiment and calculation. $k$ is the adsorption rate constant. $h$ is the initial adsorption rate constant.

with pH, indicating that CIP is not adsorbed by 0.5 mg/L AgNPs in the pH range of 5.0~9.0. In the $TiO_2$NPs-CIP binary system, the amount of CIP adsorbed onto $TiO_2$NPs increased first and then decreased with the increase of pH, which is consistent with previous result for ofloxacin adsorption to $TiO_2$NPs (Paul et al., 2012), and the maximum adsorption efficiency was 43.45% at pH = 6.5. This maximum was caused by the change in CIP species and the surface charge of $TiO_2$NPs. For example, at pH > PZC of $TiO_2$NPs (6.9), surface of $TiO_2$NPs was progressively more negatively charged with increases of pH. **Fig. 2b** shows that the content of $CIP^0$ species was approaching the peak, and $CIP^+$ species was gradually decreased with the increasing pH. This indicated the electrostatic repulsion between $TiO_2$NPs and CIP increased with an increase in pH. In the Gt-CIP binary system, the CIP adsorption achieved its maximum at pH = 6.0, and decreased when pH was higher or lower than this value, which was closed to $pK_{a1}$ (6.05) of CIP. Similar results were found for the adsorption of some organic acids (benzoic and phenylacetic, etc.), diclofenac, and flumequine onto Gt, in which the maximum adsorption amounts were obtained for pH values near their $pK_a$ of deprotonation for the carboxyl groups (Zhang and Huang, 2007; Evanko and Dzombak, 1998; Zhao et al., 2017). In addition, it was observed that the change of CIP concentration in the Gt-AgNPs-CIP and Gt-$TiO_2$NPs-CIP ternary systems with pH were similar in the Gt-CIP system, and the maximum adsorbed amount of CIP also occurred at pH=6.0. This result suggested that the presence of AgNPs or $TiO_2$NPs would not affect the trend of CIP concentration.

It was observed in **Fig. 4** that there was a significant difference between influence level of AgNPs and $TiO_2$NPs on the adsorption of CIP onto Gt under different solution pH conditions. As the solution pH increased from 5.0 to 9.0, $|\eta|$ for AgNPs gradually weakened from 16.23% to 5.33%. This is because the amount of citrate adsorbed onto Gt decreases with an increase of solution pH (Lindegren et al., 2009; Shi et al., 2010). However, when the solution pH increased from 5.0 to 6.5, $|\eta|$ for $TiO_2$NPs was almost unchanged and remained approximately 36%. Then as the solution pH dropped to 9.0, it decreased to 22.46%. The $|\eta|$ for the $TiO_2$NPs system was larger than that for the AgNPs system under the same solution pH, but the concentration of $TiO_2$NPs was 1000 times higher than that of the AgNPs system at this time. When AgNPs and $TiO_2$NPs concentrations were both 0.5 mg/L, $|\eta|$ for the $TiO_2$NPs system was

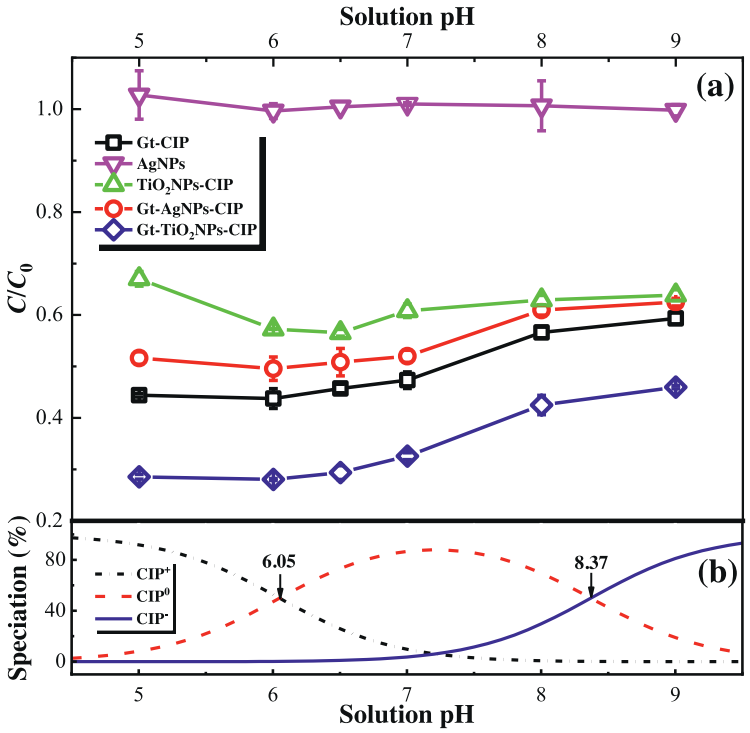


**Fig. 3 – (a): Effect of solution pH on CIP adsorption under different conditions ($C_0$ and C are CIP concentrations in aqueous-phase at initial time and after reaction, error bars represent standard deviation of $n = 3$ measurements); (b): Aqueous speciation of CIP ($pK_{a1}$=6.05 and $pK_{a2}$=8.37). The concentrations of CIP, AgNPs and $TiO_2$NPs are 0.5 mg/L, 0.5 mg/L and 500 mg/L, respectively, the background electrolyte is 0.1 mol/L NaCl, and the suspension density of Gt is 1 g/L.**

smaller than that of the AgNPs system. Furthermore, $|\eta|$ for the AgNPs system at pH = 5.0~9.0 and for the $TiO_2$NPs system at pH=6.5~9.0, they both had good linear relationships with solution pH variation ($R^2$>0.94), respectively. These results indicate that solution pH plays a significant role in $|\eta|$ variation in both systems.

### 2.3. *Mechanism of CIP adsorption on Gt / $TiO_2$NPs*

It was reported that the proposed interaction mechanism between CIP and metal cations is based on the keto and carboxylic groups in the molecule, which can be well characterized by FTIR (Gu and Karthikeyan, 2005). FTIR spectra of CIP under aqueous solution and of CIP absorbed onto Gt or $TiO_2$NPs surfaces at different pH conditions were shown in **Fig. 5a**. For the spectra of aqueous CIP, when pH = 5.0, there was a weak adsorption peak at 1710 $cm^{-1}$, which was assigned to C = O stretch of carboxylic acid ($\nu_{C=O\ carboxyl}$), whereas this peak was undetectable at pH=7.0 and 9.0. This is due to deprotonation of the carboxylic group at pH>$pK_{a1}$ of 6.07 (Gu et al., 2015; Trivedi and Vasudevan, 2007). Concurrently, the intensities of adsorption peaks around 1587 ± 2 $cm^{-1}$ and 1383±3 $cm^{-1}$, related to asymmetric and symmetric stretches of the carboxylate group, $\nu_{cooas}$ and $\nu_{coos}$, respectively, were significantly strengthened with increasing pH, indicating that deprotonation is enhanced with an increase of pH (Gu et al., 2015). However, the intensity of adsorption peak at ~1272 $cm^{-1}$, coupled the carboxylic models ($\nu_{COOH}/\delta_{C-OH}$), was observed to weaken with deprotonation of carboxyl groups, which is also consist with previously published results (Trivedi and Vasudevan, 2007). Additionally, the another adsorption peak at 1628 $cm^{-1}$ assigned to C=O stretch at quinoline ring ($\nu_{C=O\ ketone}$), was almost unchanged in intensity with pH variation (Gu and Karthikeyan, 2005).

Compared with the corresponding spectra of aqueous CIP, the position of $\nu_{coos}$ in spectra of Gt-CIP or $TiO_2$NPs-CIP was almost invariable, respectively, while the position of $\nu_{cooas}$ shifed to lower wavenumbers throughout the variations in pH conditions, as shown in Fig. 5a and Table 3. Value of $\Delta\nu = \nu_{cooas} - \nu_{coos}$ was used to elucidate the complexation model of carboxylic group and metal ions, and the results indicated a monodentate complex when a $\Delta\nu$ of carboxylate-metal complex was greater than the free carboxylate species, and otherwise the a bidentate chelate was identified (Deacon and Phillips, 1980; Tackett, 1989; Nara et al., 1996). It can be clearly observed from Table 3 that $\Delta\nu_{Gt-CIP}$ and $\Delta\nu_{TiO_2-CIP}$ were also less than those of $\Delta\nu_{CIP}$ at all pH conditions, which suggested that there was a bidentate chelate between carboxylic group of CIP and Fe(III) on the Gt or Ti(IV) on $TiO_2$NPs surfaces. Furthermore, adsorption peaks of $\nu_{C=O\ ketone}$ in Gt-CIP or $TiO_2$NPs-CIP spectra increased in strength and width compared to the spectra of aqueous CIP at all pH conditions, indicating the presence of hydrogen bonding or the coordination of the carbonyl group (Paul et al., 2012). Those results confirmed that the models of CIP adsorption by Gt and $TiO_2$NPs followed the identical mechanism, which indicated a tridentate adsorption mode involving the bidentate inner-sphere coordination of the deprotonated carboxylic group and hydrogen bonding through the

**Table 3 – The FT-IR results including the difference frequency $\Delta\nu$ of the CIP alone, Gt-CIP, and $TiO_2$NPs-CIP systems.**

| pH | CIP | | | Gt-CIP | | | $TiO_2$NPs-CIP | | |
|---|---|---|---|---|---|---|---|---|---|
| | $\nu_{COO\ as}$ | $\nu_{COO\ s}$ | $\Delta\nu$ | $\nu_{COO\ as}$ | $\nu_{COO\ s}$ | $\Delta\nu$ | $\nu_{COO\ as}$ | $\nu_{COO\ s}$ | $\Delta\nu$ |
| 5 | 1589 | 1383 | 206 | 1577 | 1383 | 194 | 1573 | 1384 | 189 |
| 7 | 1586 | 1380 | 206 | 1584 | 1380 | 204 | 1584 | 1381 | 203 |
| 9 | 1587 | 1386 | 201 | 1584 | 1385 | 199 | 1586 | 1385 | 201 |

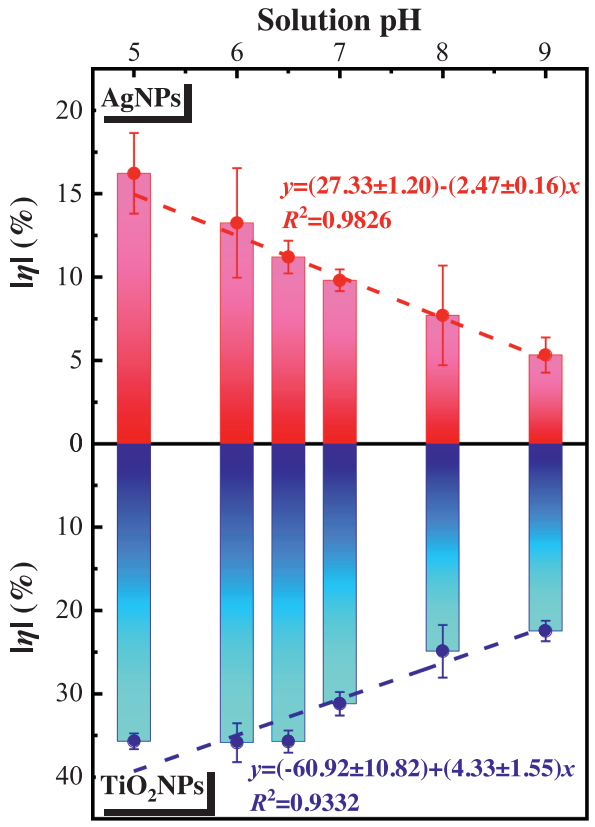


**Fig. 4 – Effect of AgNPs or $TiO_2$NPs on the difference in equilibrium concentration of CIP adsorbed to goethite under different solution pH conditions. The concentrations of CIP, AgNPs and $TiO_2$NPs are 0.5 mg/L, 0.5 mg/L and 500 mg/L, respectively, the background electrolyte is 0.1 mol/L NaCl, the suspension density of Gt is 1 g/L, and solution pH is 6.5. (The equation and dotted line is from linear regression in this figure, and error bars represent standard deviation of $n$ = 3 measurements).**

adjacent carbonyl group on the quinoline ring, as shown in Fig. 5b.

### 2.4. *Mechanism of AgNPs / $TiO_2$NPs inhibiting CIP adsorbed on Gt*

As illustrated in **Fig. 3a**, there was no adsorption between CIP and 0.5 mg/L AgNPs at the pH range of 5.0~9.0. The reason why AgNPs inhibited CIP adsorbed on Gt might be that citrate and AgNPs competition for a limited number of adsorption sites for CIP onto Gt. Previous results indicated that Gt and citrate could form inner/outer-sphere complex, and the citrate adsorption by Gt decreased with an increase of pH (Lindegren et al., 2009; Shi et al., 2010). Therefore, as the solution pH increased from 5.0 to 9.0, $|\eta|$ for AgNPs gradually weakened. Additionally, when the solution pH value was smaller than the PZC of Gt, AgNPs could be adsorbed on the Gt due to electrostatic interaction, which could be proven using XPS measurement to characterize the Gt-AgNPs-CIP ternary system at pH=6.5. As shown in **Fig. 6a**, when the AgNPs concentration was 0.5 mg/L, there was a weak signal of Ag 3d 5/2 in the XPS spectra of Gt. In order to improve the signal response intensity of Ag, the AgNPs concentration was increased to 20 mg/L, and the XPS was conducted at this higher concentration (**Fig. 6a**). After reaction time reached 10 min, adsorption peaks can be clearly seen in the XPS spectra of Gt about Ag 3d 3/2 and Ag 3d 5/2, at 373.8 and 367.8 eV, respectively. The peak intensity gradually increased with the extension of the reaction time. This result confirmed that AgNPs can be adsorbed on Gt. Correspondingly, previous multiphase advanced characterization studies have also substantiated that electrostatic attractions play a primary role between Gt and AgNPs (Wang et al., 2019).

As observed in Figs. 1 and 2a, the 0.5 mg/L $TiO_2$NPs introduced had almost no effect on CIP adsorption by Gt, whereas the significant inhibitory effect occurred when the concentration of $TiO_2$NPs increased to 500 mg/L, which we attribute to at least two possible processes including: (1) $TiO_2$NPs competition with Gt for CIP adsorption; (2) $TiO_2$NPs affect the chemisorption of CIP by Gt.

**Fig. 2a** showed that CIP could be quickly adsorbed by $TiO_2$NPs, which would reduce CIP concentration of solution. The data in **Fig. 6b** illustrate that the amount of CIP adsorbed onto Gt increased with the increase of CIP initial aqueous concentration. Furthermore, when solution pH was larger than 6.5, the amount of CIP adsorbed onto $TiO_2$NPs significantly reduced with the increase of pH in **Fig. 3a**. Furthermore, we observe in **Fig. 4** that $|\eta|$ for $TiO_2$NPs gradually decreased with the increase of pH. Therefore, $TiO_2$NPs can compete with Gt for CIP adsorption. Comparison of the FTIR spectra features of CIP absorbed to Gt with and without $TiO_2$NPs at different pH in **Fig. 6c** proved that there were no differences in the position of all functional groups adsorption peaks, which confirmed that $TiO_2$NPs did not change the chemisorption mechanism of CIP by Gt.

Based on the above analysis, the mechanisms of AgNPs and $TiO_2$NPs inhibiting CIP adsorption by Gt were different. The citrate coated AgNPs could compete with CIP for adsorption sites on Gt, while $TiO_2$NPs could compete with Gt for CIP adsorption.

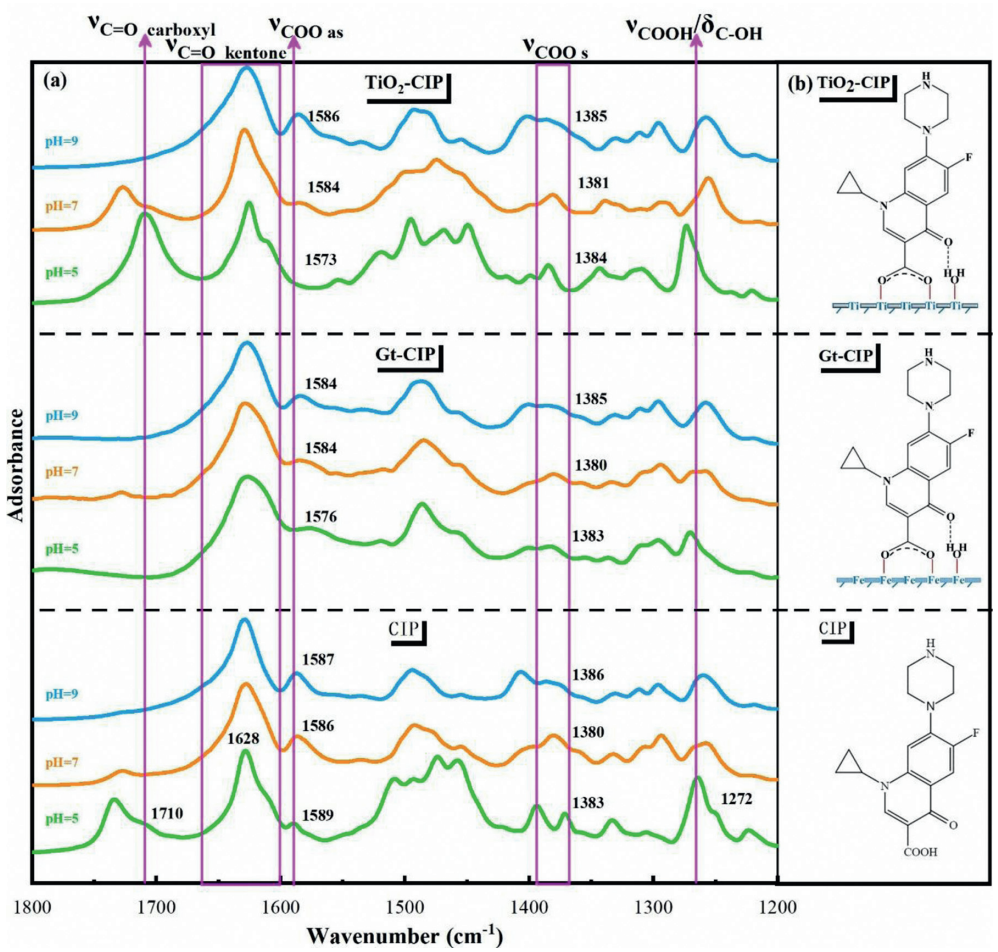


**Fig. 5 – (a): FT-IR difference spectra of CIP within aqueous solution without Gt compared to the spectra of CIP absorbed to Gt or $TiO_2$NPs at different pH values (The concentrations of CIP, AgNPs and $TiO_2$NPs are 500 mg/L, 0.5 mg/L and 500 mg/L, respectively, the background electrolyte is 0.1 mol/L NaCl, and the suspension density of Gt is 4 g/L.); (b): Proposed surface complexation species of CIP onto Gt and $TiO_2$NPs surfaces.**

### 2.5. *Environmental implications*

Adsorption of antibiotics onto Gt has been gaining interest due to increased concerns of increased occurrence, exposure, and impact of antibiotics on human health and the environment. As more and more NPs are used in various fields, antibiotics and NPs have been detected in the WWTPs and sewage sludge. This study elucidates and quantifies the FQs adsorption mechanism in the soil Gt-NPs-CIP ternary system, and sorption is critical for quantifying contaminant fate and transport when FQs and NPs enter the soil environment and migrate to the groundwater systems together. This work shows that CIP adsorption by Gt is inhibited in the presence of AgNPs or $TiO_2$NPs, but the inhibition mechanisms of AgNPs and $TiO_2$NPs are different (shown in **Fig. 7**). AgNPs could compete with CIP for adsorption sites on Gt, while $TiO_2$NPs could compete with Gt for CIP adsorption. Additionally, the inhibition impact of $TiO_2$NPs on the CIP adsorption decreased with a decrease in the concentration of $TiO_2$NPs. When $TiO_2$NPs and AgNPs both is 0.5 mg/L and also smaller concentrations, CIP can not be adsorbed by $TiO_2$NPs, and there is no difference between Gt-CIP system and Gt-$TiO_2$NPs-CIP system in terms of CIP adsorption. Therefore, these results mean that under the equal concentrations of NPs, CIP adsorption by Gt in the Gt-AgNPs-CIP system is decreased, CIP transport will not be as decreased or delayed, CIP will have increased potential for migration to groundwater, which may result in a greater risk of CIP contamination and contaminated drinking water exposure. Simultaneously, the inhibition level of AgNPs or $TiO_2$NPs was influenced by solution pH. The amount of inhibition of CIP adsorption in the Gt-AgNPs-CIP and Gt-$TiO_2$NPs-CIP system were decreased with an increase of solution pH from 5.0 to 9.0 and from 6.5 to 9.0, repectively, which suggested that the risk of groundwater contaminated by CIP increased with increasing solution pH.

## 3. Conclusions

The adsorption kinetics process of CIP by Gt can be well-captured by the pseudo-second-kinetic model, and was not significantly influenced by the presence of AgNPs or $TiO_2$NPs. Both AgNPs and $TiO_2$NPs can inhibit the adsorption of CIP by Gt. When AgNPs and $TiO_2$NPs concentrations were both 0.5 mg/L, AgNPs has a stronger inhibition effect than $TiO_2$NPs,

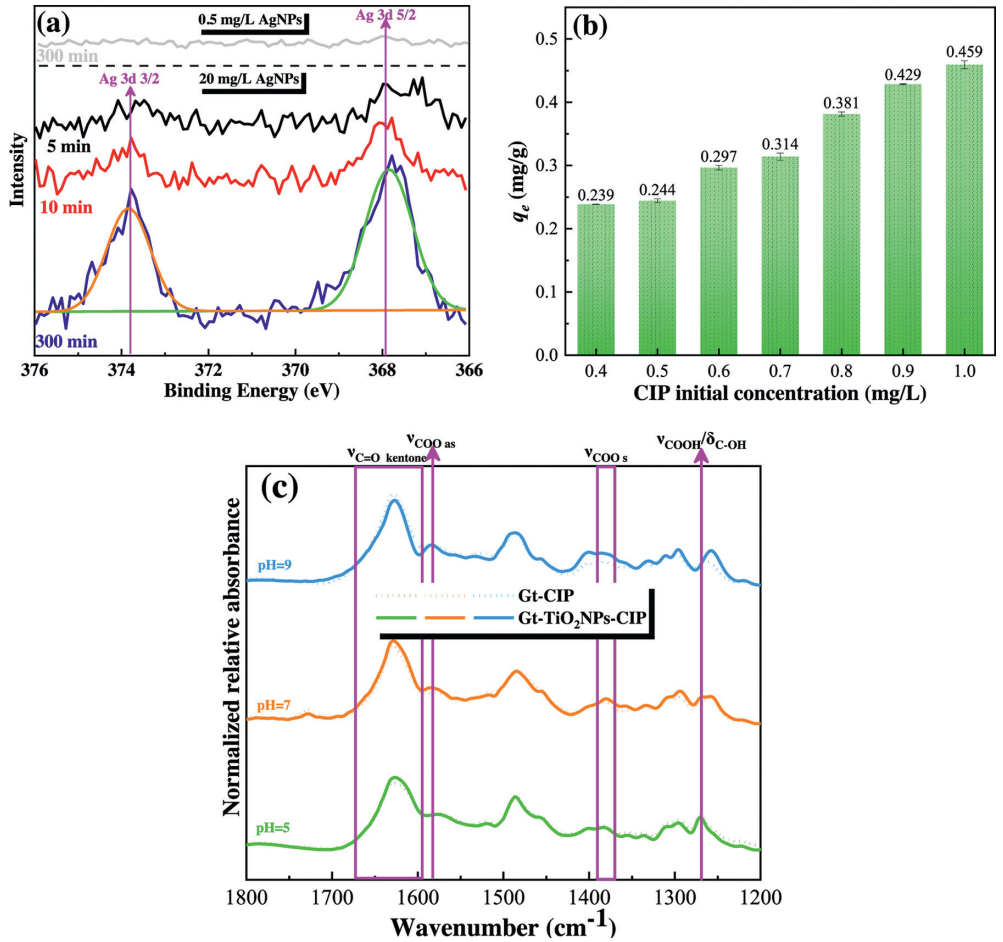


**Fig. 6 – (a) XPS spectra of Ag 3d 3/2 and Ag 3d 5/2 in the Gt-AgNPs-CIP ternary system. The concentrations of CIP is 0.5 mg/L, the concentrations of AgNPs are 0.5 mg/L or 20 mg/L, the background electrolyte is 0.1 mol/L NaCl, the suspension density of Gt is 1 g/L, and solution pH is 6.5; (b) The effect of CIP initial concentration on CIP adsorbed onto Gt. The background electrolyte is 0.1 mol/L NaCl, the suspension density of Gt is 1 g/L, and solution pH is 6.5. (error bars represent standard deviation of $n = 3$ measurements). (c) FTIR spectra features of CIP absorbed to Gt with or without $TiO_2$NPs at different pH. The concentrations of CIP and $TiO_2$NPs are 500 mg/L and 500 mg/L, respectively, the background electrolyte is 0.1 mol/L NaCl, the suspension density of Gt is 4 g/L, and solution pH is 6.5.**

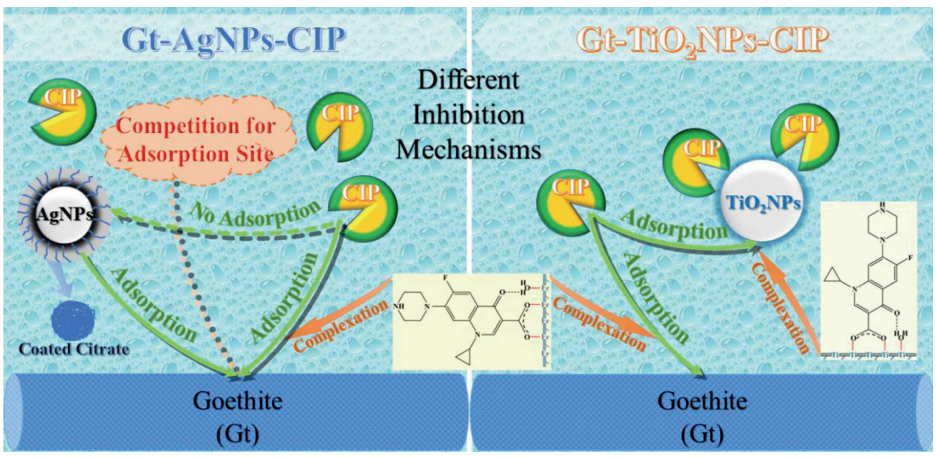


**Fig. 7 – The mechanism of CIP adsorption by Gt in presence of AgNPs or $TiO_2$NPs.**

which indicated that groundwater is more likely to be contaminated by CIP at the Gt-AgNPs-CIP system. Furthermore, the inhibition level for the AgNPs or $TiO_2$NPs system were influenced by solution pH. As the pH increased from 5.0 to 9.0, the inhibition of AgNPs on the CIP adsorption was gradually decreased from 16.23% to 5.33%. However, when the solution pH increased from 5.0 to 6.5, the inhibition of $TiO_2$NPs on the CIP adsorption was essentially unchanged at approximately 36%, and then as the solution pH increased to 9.0, it decreased to 22.46%. AgNPs and $TiO_2$NPs have different inhibition mechanisms on CIP adsorption by Gt. Citrate coated AgNPs fills the sorption sites available to CIP on Gt, and formed either inner- or outer-sphere complex under different pH conditions. However, $TiO_2$NPs and CIP could form a tridentate complex involving the bidentate inner-sphere coordination of the deprotonated carboxylic group and hydrogen bonding through the adjacent carbonyl group on the quinoline ring, which was consist with the mode of CIP adsorption by Gt. Therefore, this work has advanced our mechanistic understanding of adsorption, which is helpful to deeply understand the migration and transformation of FQs in the presence of NPs.

## Acknowledgment

This study was supported by the National Key Research and Development Program of China (No. 2020YFC1808300), the Fundamental Research Fund for the Central Universities (No. 2652019115), Guangxi Key Research Project (GuikeAB18050026), and the Natural Science Foundation of China (No. 41731282).

## REFERENCES

Bundschuh, M., Filser, J., Luderwald, S., McKee, M.S., Metreveli, G., Schaumann, G.E., et al., 2018. Nanoparticles in the environment: where do we come from, where do we go to? Environ Sci. Eur. 30.

Coulibaly, G.N., Rtimi, S., Assadi, A.A., Hanna, K., 2020. Nano-sized iron oxides supported on polyester textile to remove fluoroquinolones in hospital wastewater. Environ. Sci. Nano. 7, 2156–2165.

Davis, R., Markham, A., Balfour, J.A., 1996. Ciprofloxacin. Drugs 51, 1019–1074.

Deacon, G.B., Phillips, R.J., 1980. Relationships between the carbon-oxygen stretching frequencies of carboxylato complexes and the type of carboxylate coordination. Coord. Chem. Rev. 33, 227–250.

Deng, H., McShan, D., Zhang, Y., Sinha, S.S., Arslan, Z., Ray, P.C., et al., 2016. Mechanistic study of the synergistic antibacterial activity of combined silver nanoparticles and common antibiotics. Environ. Sci. Technol. 50, 8840–8848.

El Badawy, A.M., Silva, R.G., Morris, B., Scheckel, K.G., Suidan, M.T., Tolaymat, T.M., 2011. Surface charge-dependent toxicity of silver nanoparticles. Environ. Sci. Technol. 45, 283–287.

Evanko, C.R., Dzombak, D.A., 1998. Influence of structural features on sorption of NOM-analogue organic acids to goethite. Environ. Sci. Technol. 32, 2846–2855.

Golet, E.M., Alder, A.C., Hartmann, A., Ternes, T.A., Giger, W., 2001. Trace determination of fluoroquinolone antibacterial agents in solid-phase extraction urban wastewater by and liquid chromatography with fluorescence detection. Anal. Chem. 73, 3632–3638.

Gonzalez-Pleiter, M., Gonzalo, S., Rodea-Palomares, I., Leganes, F., Rosal, R., Boltes, K., et al., 2013. Toxicity of five antibiotics and their mixtures towards photosynthetic aquatic organisms: implications for environmental risk assessment. Water Res. 47, 2050–2064.

Gu, C., Karthikeyan, K.G., 2005. Sorption of the antimicrobial ciprofloxacin to aluminum and iron hydrous oxides. Environ. Sci. Technol. 39, 9166–9173.

Gu, X., Tan, Y., Tong, F., Gu, C., 2015. Surface complexation modeling of coadsorption of antibiotic ciprofloxacin and Cu(II) and onto goethite surfaces. Chem. Eng. J. 269, 113–120.

Hiemstra, T., Dewit, J.C.M., Vanriemsdijk, W.H., 1989. Multisite proton adsorption modeling at the solid-solution interface of (hydr)oxides - a new approach.2. Application to various important (hydr)oxides. J. Colloid Interface Sci. 133, 105–117.

Ho, Y.S., 2006. Review of second-order models for adsorption systems. J. Hazard. Mater. 136, 681–689.

Hu, Y., Xue, Q., Tang, J., Fan, X., Chen, H., 2019. New insights on Cr(VI) retention by Ferrihydrite in the presence of Fe(II). Chemosphere 222, 511–516.

Huang, Y.Q., Wang, Y., Huang, Y.Z., Zhang, L.X., Ye, F., Wang, J.L., et al., 2020. Impact of sediment characteristics on adsorption behavior of typical antibiotics in Lake Taihu. China Sci. Total Environ. 718, 12.

Kovalakova, P., Cizmas, L., McDonald, T.J., Marsalek, B., Feng, M., Sharma, V.K., 2020. Occurrence and toxicity of antibiotics in the aquatic environment: a review. Chemosphere 251, 126351.

Larsson, D.G.J., de Pedro, C., Paxeus, N., 2007. Effluent from drug manufactures contains extremely high levels of pharmaceuticals. J. Hazard. Mater. 148, 751–755.

Li, B., Zhang, T., 2010. Biodegradation and adsorption of antibiotics in the activated sludge process. Environ. Sci. Technol. 44, 3468–3473.

Lindegren, M., Loring, J.S., Persson, P., 2009. Molecular structures of citrate and tricarballylate adsorbed on alpha-FeOOH particles in aqueous suspensions. Langmuir 25, 10639–10647.

Martin, S., Shchukarev, A., Hanna, K., Boily, J.F., 2015. Kinetics and mechanisms of ciprofloxacin oxidation on hematite surfaces. Environ. Sci. Technol. 49, 12197–12205.

Musee, N., 2017. A model for screening and prioritizing consumer nanoproduct risks: a case study from South Africa. Environ. Int. 100, 121–131.

Mutavdzic Pavlovic, D., Curkovic, L., Grcic, I., Simic, I., Zupan, J., 2017. Isotherm, kinetic, and thermodynamic study of ciprofloxacin sorption on sediments. Environ. Sci. Pollut. Res. 24, 10091–10106.

Nara, M., Torii, H., Tasumi, M., 1996. Correlation between the vibrational frequencies of the carboxylate group and the types of its coordination to a metal Ion: an *ab initio* molecular orbital study. J. Phys. Chem. 100, 19812–19817.

Nowack, B., Bucheli, T.D., 2007. Occurrence, behavior and effects of nanoparticles in the environment. Environ. Pollut. 150, 5–22.

Oshannessy, D.J., Winzor, D.J., 1996. Interpretation of deviations from pseudo-first-order kinetic behavior in the characterization of ligand binding by biosensor technology. Anal. Biochem. 236, 275–283.

Paul, T., Dodd, M.C., Strathmann, T.J., 2010. Photolytic and photocatalytic decomposition of aqueous ciprofloxacin: transformation products and residual antibacterial activity. Water Res 44, 3121–3132.

Paul, T., Machesky, M.L., Strathmann, T.J., 2012. Surface complexation of the zwitterionic fluoroquinolone antibiotic ofloxacin to nano-anatase $TiO_2$ photocatalyst surfaces. Environ. Sci. Technol. 46, 11896–11904.

Pico, Y., Andreu, V., 2007. Fluoroquinolones in soil - risks and challenges. Anal. Bioanal. Chem. 387, 1287–1299.

Pellegrino, R.M., Segoloni, F., Cagini, C., 2008. Simultaneous determination of Ciprofloxacin and the active metabolite of Prulifloxacin in aqueous human humor by high-performance liquid chromatography. J. Pharm. Biomed. Anal. 47, 567–574.
Shi, Z., Li, F., Yao, S., 2010. Effect of small organic acid anions on the adsorption of phosphate anions onto synthetic goethite from aqueous solution. Adsorpt. Sci. Technol. 28, 885–893.
Simonin, J.P., 2016. On the comparison of pseudo-first order and pseudo-second order rate laws in the modeling of adsorption kinetics. Chem. Eng. J. 300, 254–263.
Tackett, J.E., 1989. FT-IR characterization of metal acetates in aqueous solution. Appl. Spectrosc. 43, 483–489.
Tan, Y., Guo, Y., Gu, X., Gu, C., 2014. Effects of metal cations and fulvic acid on the adsorption of ciprofloxacin onto goethite. Environ. Sci. Pollut. Res. 22, 609–617.
Trivedi, P., Vasudevan, D., 2007. Spectroscopic investigation of ciprofloxacin speciation at the goethite-water interface. Environ. Sci. Technol. 41, 3153–3158.
Tyagi, N., Kumar, A., 2020. Understanding effect of interaction of nanoparticles and antibiotics on bacteria survival under aquatic conditions: knowns and unknowns. Environ. Res. 181, 108945.
Valdes, M.E., Santos, L., Rodriguez Castro, M.C., Giorgi, A., Barcelo, D., Rodriguez-Mozaz, S., et al., 2021. Distribution of antibiotics in water, sediments and biofilm in an urban river (Cordoba, Argentina, LA). Environ. Pollut. 269, 116133.
Van Doorslaer, X., Dewulf, J., Van Langenhove, H., Demeestere, K., 2014. Fluoroquinolone antibiotics: an emerging class of environmental micropollutants. Sci. Total Environ. 500, 250–269.
Van Wieren, E.M., Seymour, M.D., Peterson, J.W., 2012. Interaction of the fluoroquinolone antibiotic, ofloxacin, with titanium oxide nanoparticles in water: adsorption and breakdown. Sci. Total Environ. 441, 1–9.
Wang, C.J., Li, Z.H., Jiang, W.T., Jean, J.S., Liu, C.C., 2010. Cation exchange interaction between antibiotic ciprofloxacin and montmorillonite. J. Hazard. Mater. 183, 309–314.
Wang, R., Dang, F., Liu, C., Wang, D.J., Cui, P.X., Yan, H.J., et al., 2019. Heteroaggregation and dissolution of silver nanoparticles by iron oxide colloids under environmentally relevant conditions. Environ. Sci. Nano 6, 195–206.
Wu, M., Zhao, S., Jing, R., Shao, Y., Liu, X., Lv, F., et al., 2019. Competitive adsorption of antibiotic tetracycline and ciprofloxacin on montmorillonite. Appl. Clay Sci. 180, 105175.
Yang, X., Zhang, C., Liu, F., Tang, J., Huang, F., Zhang, L., 2019. Diversity in the species and fate of chlorine during TCE reduction by two nZVI with non-identical anaerobic corrosion mechanism. Chemosphere 230, 230–238.
Zhang, H., Huang, C.H., 2007. Adsorption and oxidation of fluoroquinolone antibacterial agents and structurally related amines with goethite. Chemosphere 66, 1502–1512.
Zhang, H., Khanal, S.K., Jia, Y., Song, S., Lu, H., 2019a. Fundamental insights into ciprofloxacin adsorption by sulfate-reducing bacteria sludge: mechanisms and thermodynamics. Chem. Eng. J. 378, 122103.
Zhang, M., Yang, J., Cai, Z., Feng, Y., Wang, Y., Zhang, D., Pan, X., 2019b. Detection of engineered nanoparticles in aquatic environments: current status and challenges in enrichment, separation, and analysis. Environ. Sci. Nano 6, 709–735.
Zhao, Y., Liu, F., Qin, X., 2017. Adsorption of diclofenac onto goethite: adsorption kinetics and effects of pH. Chemosphere 180, 373–378.
Zhou, L., Martin, S., Cheng, W., Lassabatere, L., Boily, J.F., Hanna, K., 2019. Water flow variability affects adsorption and oxidation of ciprofloxacin onto hematite. Environ. Sci. Technol. 53, 10102–10109.